

Specific Absorption Rate Evaluation in a Typical Multilayer Fruit: Coconut with Twig due to Electromagnetic Radiation as per Indian Standards

Ardhendu Kundu¹, Bhaskar Gupta¹, and Amirul I. Mallick²

Abstract – Specific Absorption Rate (SAR) is a common technical specification tagged to devices like mobile phones, voice-calling tabs etc. that utilize electromagnetic energy for communication. However, SAR limits are prescribed only for safety of humans from adverse biological effects mediated by Radio Frequency (RF) radiation. On the other hand, very few reports are available to visualize the gross effect of RF energy absorption in plants and vegetables that are continuously exposed to electromagnetic radiation from cell phone towers and Wi-Fi antennas throughout their lifespan. Most fruits and plants have moderately high permittivity (ϵ') and electrical conductivity (σ) that result in reasonable amount of RF energy absorption among them. Measured dielectric properties for different coconut (*Cocos nucifera*) layers have been reported in this article along with analysis of open ended coaxial probe technique for dielectric characterization. Next, RF energy absorption in a typical twig connected multilayer coconut structure has been reported in context with Indian reference levels. SAR value is highly dependent on geometry of the dielectric body and in real time scenario, there is a twig attached to every coconut that not only modifies SAR distribution but also increases SAR value due to its sharp geometry. In addition, SAR data for this multilayer twig connected coconut have been evaluated as per revised Indian RF exposure standards that replicate the existing scenario in India. SAR values are evaluated based on finite integration technique due to linearly polarized plane wave exposure at 947.5 MHz (935-960 MHz downlink band), 1842.5 MHz (1805-1880 MHz downlink band) and 2450 MHz (2400-2500 MHz band) in public places only.

Keywords – Coconut, Dielectric properties, Radio Frequency (RF), Revised Indian RF Exposure Standards, Linearly Polarized Plane Wave, Specific Absorption Rate (SAR).

I. INTRODUCTION

Analysis of electromagnetic wave propagation and Radio Frequency (RF) energy absorption in living objects starts with dielectric characterization of biological tissues i.e. permittivity (ϵ') and loss tangent ($\sigma/\omega\epsilon_0\epsilon'$) measurement. Once dielectric characterization is done, field propagation data in biological tissue medium can be calculated using numerical techniques based on Maxwell's equations [1]. Specific Absorption Rate

Article history: Received December 16, 2016; Accepted December 07, 2017

¹Ardhendu Kundu[#] and Bhaskar Gupta are with Electronics and Telecommunication Engineering Department, Jadavpur University, Kolkata 700 032, India, E-mail: [#]ardhendukundu.1989@gmail.com, gupta_bh@yahoo.com

²Amirul I. Mallick is with Department of Biological Sciences, IISER Kolkata, West Bengal 741246, India, E-mail: amallick@iiserkol.ac.in

(SAR) is defined as measure of the rate at which Radio Frequency (RF) energy is absorbed by a dielectric mass when exposed to an electromagnetic field with unit of watts per kilogram (W/Kg) or milliwatts per gram (mW/g). A number of articles are available in literature on biological effects due to electromagnetic exposure and SAR measurements in humans due to RF exposure from different sources [2-15]. In 2004, Balmori reported long term effects of cell tower radiation on plants like notable health deterioration, high susceptibility to illness and slower growth rate etc. [2]. In 2010, Panagopoulos et al. reported reduced reproductive capability in adult *Drosophila melanogaster* while exposed to GSM band radiation [3]. In the same year, Girish Kumar has also reported several cancer cases near cell towers and reduced productivity in fruit bearing trees due to non-ionizing radiation [4]. Sivani and Sudarsanam showed that microwave exposure can have effects on neurotransmitter functions, blood-brain barrier, cellular metabolism, and gene / protein expression in certain cells even at lower intensity levels (2013) [5]. In addition, several researchers have reported RF energy absorption in human head / body phantom model [6] and variation in RF energy absorption for different human head models and tissue composition [7-8], along with minimum distance from GSM base stations to comply with RF exposure guidelines [9]. Electromagnetic energy absorption in eye, testis, brain and kidney has also been reported in literature (2006) [10]. Hirata et al. have reported that electrical tissue characteristics and phantom surface area are two dominant factors that influence whole body averaged SAR value (2007) [11]. SAR simulation in nine months old Japanese infant and practical SAR measurement systems in flat phantom were reported in literature (2008) [12-13]. SAR analysis and consequent temperature increment in human head and eye model have also been reported in literature [14-15]. Depending upon the findings on probable biological effects of RF radiation on humans, different RF exposure guidelines have been prepared by organizations like International Commission on Non-Ionizing Radiation Protection (ICNIRP), Federal Communications Commission (FCC) and Department of Telecommunications (DoT), India and adopted worldwide [16-18]. However, much stricter guidelines have also been adopted in many other countries like Switzerland, Italy, Poland and Luxembourg etc. to avoid suspected biological hazards of RF exposure [4, 19]. SAR is considered as the metric for quantifying RF energy absorption in human body as prescribed in several RF exposure guidelines mentioned earlier [16-18]. SAR is usually averaged either over a small sample volume typically point mass / 1-g (adopted by FCC and DoT) / 10-g (adopted by ICNIRP) of tissue or over the

whole body. SAR to a great extent depends on geometry and orientation of the dielectric body that is exposed to electromagnetic field. Mathematically, local point SAR is calculated following relation illustrated in Eq. (1).

$$SAR = \frac{\sigma E^2}{2\rho} \quad (1)$$

where: σ is the conductivity of tissue dielectric layer, E is electric field (peak) inside tissue dielectric layer, and ρ is the material density of tissue dielectric layer.

SAR is specified for human exposure to electromagnetic fields up to 10 GHz as per ICNIRP guidelines whereas the same is prescribed only up to 6 GHz as per FCC guidelines [16-17]. Indian RF exposure standards have been revised on 1st September, 2012. Revised Indian RF exposure standards reduce the maximum permissible RF power density to 1/10th of ICNIRP guidelines (at public zone) whereby maximum permissible SAR value is reduced to 1.6 W/Kg averaged over 1-g of contiguous human tissue [18].

Plants and vegetables are exposed to electromagnetic radiation throughout their lifespan from mobile towers and Wi-Fi antennas. Unfortunately till date there are no national or international RF exposure guidelines and SAR limits prescribed for their safety. Nowadays researchers along with ground level peasants are claiming that plant health and fruit production is also affected at intense radio frequency radiation zones near cell towers [2, 4, 20-30]. In 2010, G. Kumar submitted a report that summarizes reduced seed germination and root growth in plants due to radio frequency exposure [4]. Earlier in 1996, scientists have reported a significant negative correlation between radial growth of pine trees and electric field intensity [20]. Even developmental abnormalities have been observed in offsprings of microwave exposed plants along with reduced life span of daughter plants (1996) [21].

In 2009, Balmori summarized several physiological and genetic effects of RF radiation on plants [22]. Chlorophyll concentrations have been quantitatively studied in leaves of black locust (*Robinia pseudoacacia L.*) seedlings exposed to high frequency electromagnetic fields of 400 MHz; logarithmically decreased ratio of the two main types of chlorophyll has been reported with increase of daily RF exposure time [22-23]. Even, 900 MHz RF exposed tomato plants have expressed abundance of three specific genes with respect to control; the same is considered to be injurious stimulation [22]. In a recent study, significant reduction in *Capsicum annuum* seed germination is reported while exposed to GSM cell phone radiation over 50 days [24]. On the other hand, some recent articles are available in literature dealing with RF energy absorption / SAR investigation in Indian fruits due to electromagnetic radiation absorption [25-30].

Coconut (*Cocos nucifera*) water is considered to be one of the richest natural health drinks all over the world [31]. Dried brown scratches are observed on green skin of coconuts during last 15-20 years at several places in India. Hence it is important to investigate whether these brown scratches on

green coconut are formed due to exposure to cell tower emitted microwave radiation or not. An article is available in literature that investigates SAR in simpler coconut structures without considering the twig as per ICNIRP RF exposure norms [26]. However SAR distribution is significantly dependent upon geometry of dielectric tissue that is exposed to RF radiation; therefore considering the twig (a cone like geometry with large height to radius ratio) connected to coconut structure would definitely provide a more accurate SAR measurement replicating real time scenario. In addition, SAR values have been evaluated following revised Indian RF exposure standards at respective center frequencies of 935-960 MHz downlink band, 1805-1880 MHz downlink band and 2400-2500 MHz band [18].

An accurate multilayer twig connected coconut has been modelled using CST MWS 2010 platform [32]. The coconut model consists of four different sections i.e. sharp twig, green skin (Exocarp), yellowish pulp (Mesocarp) and coconut water (Liquid Endosperm). Dielectric properties and material densities have been measured for green skin, yellowish pulp, coconut water and sharp twig is assumed to have similar dielectric properties to green skin. Maximum Local point SAR (MLP-SAR) and 1-g averaged SAR values have been simulated for linearly polarized plane wave exposures following revised Indian RF exposure standards at 947.5 MHz, 1842.5 MHz and Wi-Fi 2450 MHz. 10-g averaged SAR values have also been evaluated in all cases though the same is not considered in revised Indian RF exposure standards. Three dimensional point and 1-g averaged SAR distributions have also been investigated to determine SAR values exactly at junction point where the twig is attached to coconut.

II. BROADBAND DIELECTRIC PROPERTIES MEASUREMENT OF DIFFERENT LAYERS IN COCONUT

There are several alternatives like cavity perturbation technique, waveguide and coaxial transmission line technique, free space transmission technique, time domain reflectometry technique, microstrip transmission line technique and open ended coaxial probe technique etc. for dielectric properties measurement of solid, semi-solid and liquid samples [33-34]. Among the above mentioned alternatives, open ended coaxial probe technique is widely used for dielectric characterization of biological tissues (Stuchly et al. and other groups) [35-44]. Therefore, open ended coaxial probe technique has been pursued for characterizing dielectric properties of different coconut layers.

However before detailing measured dielectric data, physics behind this dielectric characterization technique should be highlighted. Open ended coaxial probe can be represented by a fringing capacitance from inner to outer conductor out of the coaxial structure through biological tissue medium and radiation conductance that represents propagation loss through biological medium as illustrated in Fig. 1. In addition, there is another fringing capacitance from inner to outer conductor within the coaxial structure through the intervening material

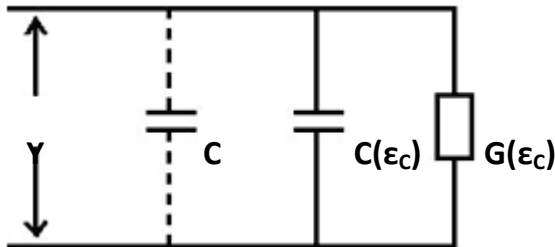


Fig. 1 Equivalent circuit diagram of an open ended coaxial probe

[35-44]. The capacitance and conductance are dependent on frequency of measurement and complex dielectric properties of biological sample for a probe with known dimensions. Input admittance of the probe model can be expressed by Eq. (2).

$$Y = G(\epsilon_c, \omega) + j\omega C(\epsilon_c, \omega) \quad (2)$$

$$Y_0 = G_0(1, \omega) + j\omega C_0(1, \omega) \quad (2a)$$

Y_0 is input admittance of the probe in air/ vacuum

G_0 is conductance while the probe is in air / vacuum

C_0 is capaticance while the probe is in air/vacuum

ϵ_c is complex permittivity of biological sample

ω is angular frequency

Open ended coaxial probe can be analytically modelled as an antenna in a lossy medium.

$$Y(\epsilon_c, \omega) = \sqrt{\epsilon_c} Y_0(1, \omega \sqrt{\epsilon_c}) \quad (3)$$

$$Y = j\omega \epsilon_c C_0 + \sqrt{\epsilon_c} G_0 \quad (3a)$$

According to Deschamps's theorem, Eq. 3 interprets that input admittance of the probe in medium with complex permittivity ϵ_c at an angular frequency ω is equivalent to the input admittance of the probe in vacuum at angular frequency $\omega \sqrt{\epsilon_c}$ and furthermore multiplied by $\sqrt{\epsilon_c}$ [35].

Capacitance C_0 can be considered constant in free space; however, radiation conductance G_0 when the antenna (open ended coaxial probe) is in vacuum can be calculated using formula derived by Liu (1986) and illustrated in Eqs. (4) to (4c) [36-37]. The Bessel function can be expanded using Maclaurin series,

$$G_0 = \left[\frac{Y_0}{\ln\left(\frac{a}{b}\right)} \right] \int_0^{\pi/2} [J_0(ka \sin \theta) - J_0(kb \sin \theta)]^2 \frac{d\theta}{\sin \theta} \quad (4)$$

$$G_0 \approx \left[\frac{Y_0}{\ln\left(\frac{a}{b}\right)} \right] [G_1(\omega^4) + G_2(\omega^6) + \dots] \quad (4a)$$

$$G_0 \approx \left[\frac{Y_0}{\ln\left(\frac{a}{b}\right)} \right] [G_1(\omega^4)] \quad (\text{for N type/ SMA connectors}) \quad (4b)$$

$$G_0 \propto \omega^4 \quad (4c)$$

$J_0(x)$ is the Bessel function and G_1, G_2, \dots etc. are parameters that depend on antenna dimensions like a (inner radius of outer conductor), b (outer radius of inner conductor) and frequency of operation. k is equal to $2\pi/\lambda_0$ where λ_0 stands for free space wavelength. It has been found that G_0 can be approximated by G_1 for N type and SMA connectors. Hence, radiation conductance of coaxial probe can be considered to be varying with ω^4 [36-37].

Simplifying Eqs. (2) and (3), expression derived for input admittance is presented in Eq. (3a). Y is the measured input admittance of the probe whereas C_0 and G_0 are capacitance and radiation conductance of the probe antenna in free space respectively.

Input admittance of the coaxial probe Y is related to the measured reflection coefficient S_{11} (in linear scale) by Eq. (5) [43].

$$Y = Y_0 \frac{1-S_{11}}{1+S_{11}} \quad (5)$$

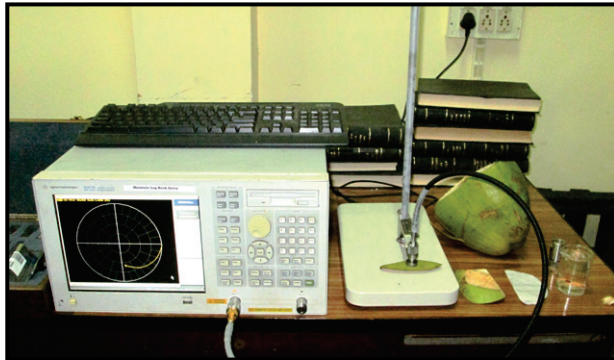
where, $Y_0 = 1/50\Omega = 0.02 S$

(characteristics admittance of the coaxial probe)

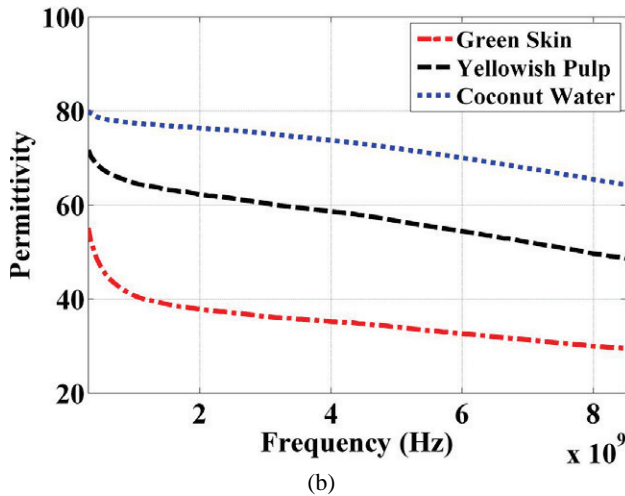
While input admittance (Y) is calculated from reflection coefficient (S_{11} in linear scale) parameter, following steps are considered to characterize the unknown tissue dielectric sample.

- a. Complex input admittance (Y) illustrated in Eq. (3a) is split into real and imaginary parts.
- b. Two nonlinear equations are obtained from Eq. (3a) for two unknowns C_0 and G_0 respectively.
- c. For obtaining C_0 and G_0 , first complex input admittance (Y) is measured for a sample (like distilled water) with known complex permittivity during calibration. Measured value for complex input admittance (Y) and known complex permittivity of the reference dielectric material are put in Eq. (3a). Then C_0 and G_0 are easily solved using Eq. (3a).
- d. While C_0 and G_0 are solved after calibration, complex permittivity for any unknown tissue sample can be obtained by putting values for measured input admittance (Y) and C_0 , G_0 in Eq. (3a).

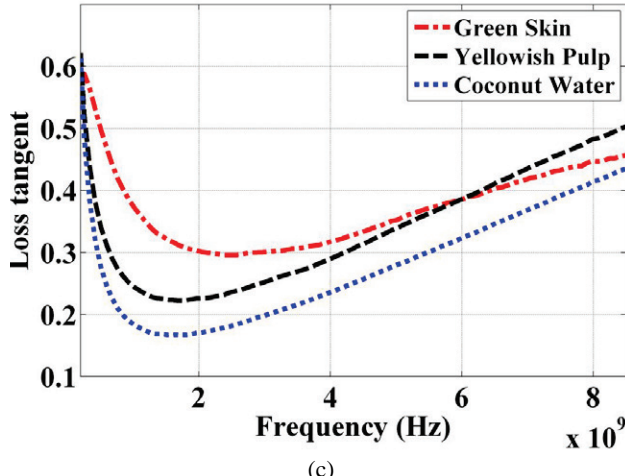
Agilent 85070E dielectric probe kit is a standard version of open ended coaxial probe technique for dielectric measurement. It contains a high temperature coaxial probe (up to 200°C) that can measure permittivity (ϵ') and loss tangent ($\tan \delta$) from amplitude and phase of the reflected signal at surface of material under test after proper calibration. A Vector Network Analyzer (VNA) is required during the open-short-distilled water calibration procedure for coaxial probe [25, 27-30]. The dielectric properties measurement set up is illustrated in Fig. 2a.



(a)



(b)



(c)

Fig. 2. (a) Dielectric parameter measurement set up with open ended dielectric probe and VNA (b) Permittivity (ϵ') plot for three different layers in coconut (c) Loss Tangent ($\tan \delta$) plot for three different layers in coconut

Dielectric parameters for three different coconut layers have been measured up to 8.5 GHz due to frequency limitation of VNA. Dielectric properties for sharp twig couldn't be measured alone using open ended coaxial probe (2 cm diameter) as the twig is very thin. Therefore, dielectric properties for twig have been considered to be same with green skin[#]. Measured permittivity and loss parameters for different coconut layers are illustrated in Figs. 2b and 2c respectively. In addition to graphical illustrations, dielectric parameters at 947.5 MHz, 1842.5 MHz and 2450 MHz have been tabulated in Table I.

TABLE I
DIELECTRIC PARAMETER MEASUREMENT OF DIFFERENT LAYERS IN GREEN COCONUT

Name of fruit	947.5 MHz		1842.5 MHz		2450 MHz	
	ϵ'	$\tan \delta$	ϵ'	$\tan \delta$	ϵ'	$\tan \delta$
Green skin	41.21	0.385	38.12	0.306	37.14	0.296
Yellowish pulp	65.01	0.251	62.59	0.224	61.46	0.235
Coconut water	77.54	0.190	76.51	0.168	75.91	0.181
Twig [#]	41.21	0.385	38.12	0.306	37.14	0.296

TABLE II
MODELLING SPECIFICATIONS FOR TWIG CONNECTED COCONUT STRUCTURE

Name of the layer	Sections required to construct the layer	Least thickness of the layer [cm]	Volume of the layer [cm ³]	Mass of the layer [Kg]
Green skin	Cone + sphere + cylinder + sphere + cone	0.5	285.870	0.304166
Yellowish Pulp	Cone + sphere + cylinder + sphere + cone	2.5	745.124	0.727241
Coconut water	Sphere + cylinder + sphere	3.5	327.801	0.332062
Twig	Cone	0.1	4.47086	0.004757

III. COCONUT MODELLING AND SAR COMPUTATIONAL METHOD

A. Coconut Modelling

Initially a typical standard size fresh coconut (*Cocos nucifera*) of 1.40 Kg mass has been collected from market to observe shape of coconut, shape of connecting twig, number of distinguishable layers in coconut structure, thickness of each layer along with their inner/outer dimensions etc. Reviewing detailed geometry of coconut, shape of twig connected coconut and size of different sections; three different dielectric layers have been identified from outer to inner direction and named as green skin (Exocarp), yellowish pulp (Mesocarp) and coconut water (Liquid Endosperm). Hard shell (Endocarp) dielectric layer is so thin that the same couldn't be characterized as a separate dielectric layer due to difficulties in measuring accurate dielectric parameters with open ended coaxial probe technique that asks for a minimum dielectric thickness (dependent on skin depth) for accurate measurement [35-44]. Therefore, the hard shell (Endocarp) has been taken into consideration along with yellowish pulp (Mesocarp) region. Besides these three layers, the twig connected with coconut has been considered as a separate section; consideration of twig in coconut structure improves SAR estimation over the previous coconut SAR evaluation work available in literature [26].

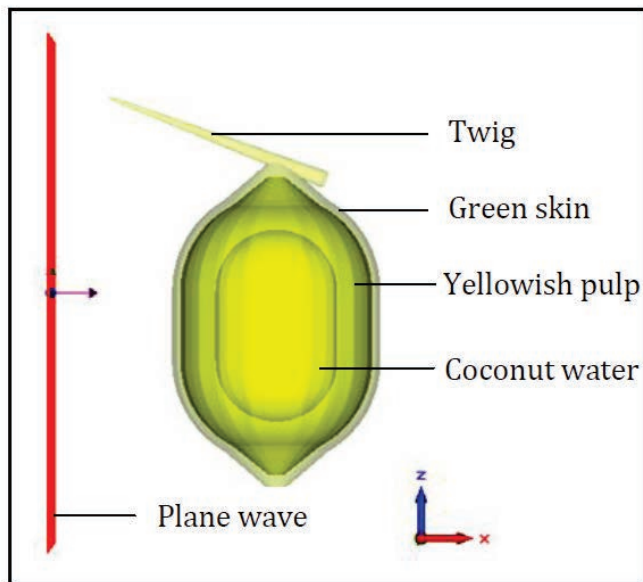


Fig. 3 Twig connected coconut fruit modelled in CST-MWS platform

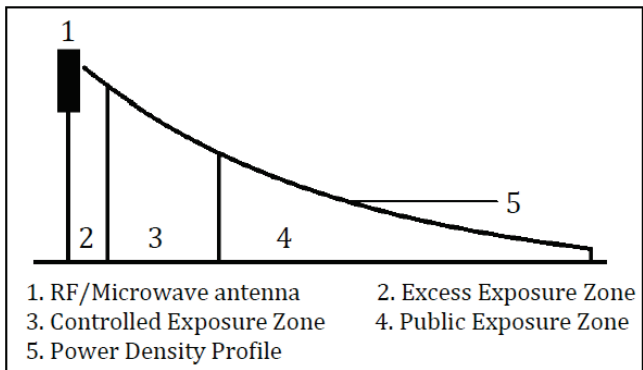


Fig. 4 RF exposure zones around a base station antenna

The twig connected three-layer coconut structure has been modelled in CST-MWS 2010 software with proper dimensions for each layer; a sharp twig has been newly incorporated for more accurate SAR estimation over available work in literature [26]. Designed typical twig connected multilayer coconut model is illustrated in Fig. 3 along with detailed modelling specifications tabulated in Table II.

B. SAR Computational Method

SAR computation method for twig connected coconut structure is exactly similar to the earlier technique illustrated in literature for simplified coconut and other fruit structures [25-30]. This time a three layer coconut model with an additional twig is designed in CST-MWS 2010 [32]. Three coconut layers from outer to inner direction are top most green skin (Exocarp), intermediate yellowish pulp (Mesocarp) and inner most coconut water (Liquid Endosperm) along with

a twig structure physically connected to one pole of coconut on green skin. Dielectric properties and material densities have been defined for each section. A linearly polarized plane wave impinges on twig connected coconut structure in time domain solver; however, plane wave field strength varies with frequency of exposure. A typical Gaussian pulse of around 100 ns duration has been used for excitation. A 4-layered Perfectly Matched Layer (PML) has been used as absorbing boundary with 0.0001 reflection coefficient. Distance between coconut structure and plane wave has been kept fixed at 3 cm by varying mesh settings at different frequencies of exposure.

IV. REVISED INDIAN RF EXPOSURE STANDARDS AND CALCULATED SAR RESULTS IN TWIG CONNECTED COCONUT STRUCTURE

In this research work, not only a twig has been incorporated along with the coconut structure for more accurate SAR estimation but also RF exposure levels have been set as per revised Indian RF exposure standards [18]. These two factors lead to an accurate SAR estimation for real coconut structure in present Indian circumstances. Before discussing SAR results for twig connected coconut structure at 947.5 MHz, 1842.5 MHz and 2450 MHz, it is more important to throw some light on revised Indian RF exposure standards.

A. Overview on Revised Indian RF Exposure Standards

ICNIRP RF exposure guidelines were in effect in India up to 31st August 2012 along with many other European countries [16]. However, Department of Telecommunications (DoT), India has revised safe limits of radio frequency exposure to stricter values for all frequencies up to 300 GHz [18]. There are mainly three RF exposure zones around a base station RF/microwave antenna; they are named as Excess exposure zone, Controlled exposure zone and Public exposure zone. These three RF exposure zones are pointed out in Fig. 4 along with RF/microwave antenna and power density profile. As per revised Indian RF exposure standards, maximum permissible RF power densities at public zones have been reduced to 1/10th of ICNIRP guidelines but nothing has been mentioned for excess and controlled RF exposure zones. This implies that maximum permissible RF power densities have been kept unchanged for those two zones. Accordingly, maximum permissible RF exposure limits for public zone have been tabulated in Table III. In addition to the RF exposure reference levels, revised Indian RF exposure standards also include basic restriction on maximum permissible SAR limit up to 1.6 W/Kg averaged over 1-g of contiguous human tissue [18]. However, it should be noted that all these RF exposure standards and SAR limits are prescribed for humans only and they are not at all applicable for plants, vegetables or fruits.

B. Calculated SAR Results in Twig Connected Coconut Structure

SAR investigations have been performed for twig connected coconut structure due to linearly polarized plane wave exposure at public zone; SAR data have been simulated at 947.5 MHz (935-960 MHz downlink band), 1842.5 MHz (1805-1880 MHz downlink band) and 2450 MHz (2400-2500 MHz band) as per revised Indian RF exposure standards. CST-MWS 2010 simulator works with peak E-field vector of linearly polarized plane wave and therefore, peak E-field values are obtained by multiplying the unperturbed r. m. s. E-field values by $\sqrt{2}$ (considering sinusoidal variation) at each three frequencies of interest and tabulated in Table III. This implies that the typical coconut is exposed to linearly polarized plane waves exactly as per revised Indian RF exposure standards in all three frequency bands. In real time scenario, plane waves from cell tower and Wi-Fi antennas get radiated 24 hours a day and 365 days a year, hence calculated SAR values would not reduce by averaging over longer time

TABLE III
SAR RESULTS FOR TWIG CONNECTED COCONUT WITH
E-FIELD SET AS PER REVISED INDIAN RF EXPOSURE
STANDARDS

Peak E-field value of the plane wave [V/m]	Frequency of operation [GHz]	SAR Averaging	Simulated max SAR [W/kg] (r. m. s)	Total SAR [W/kg] (r. m. s)
18.90	0.9475	Point	0.260	0.0056
"	"	1	0.072	"
"	"	10	0.024	"
26.36	1.8425	Point	0.689	0.0107
"	"	1	0.184	"
"	"	10	0.084	"
27.46	2.45	Point	1.039	0.0107
"	"	1	0.236	"
"	"	10	0.104	"

SAR distribution for coconut model (W/Kg)

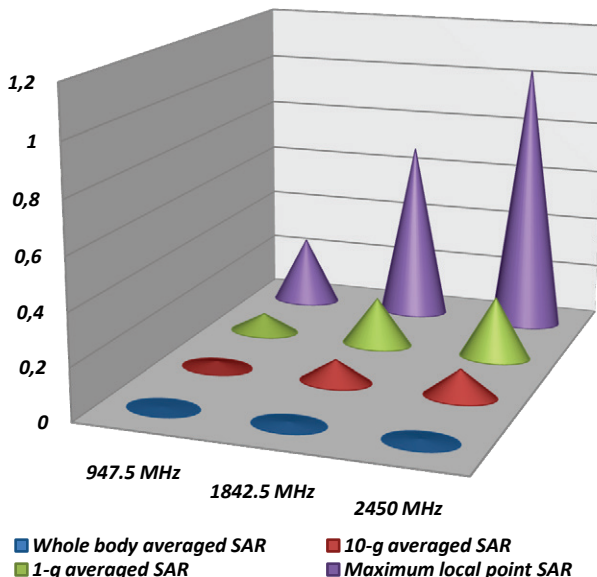


Fig. 5 Comparative SAR analysis for twig connected coconut structure at 947.5 MHz, 1842.5 MHz and 2450 MHz as per current electromagnetic standards in India

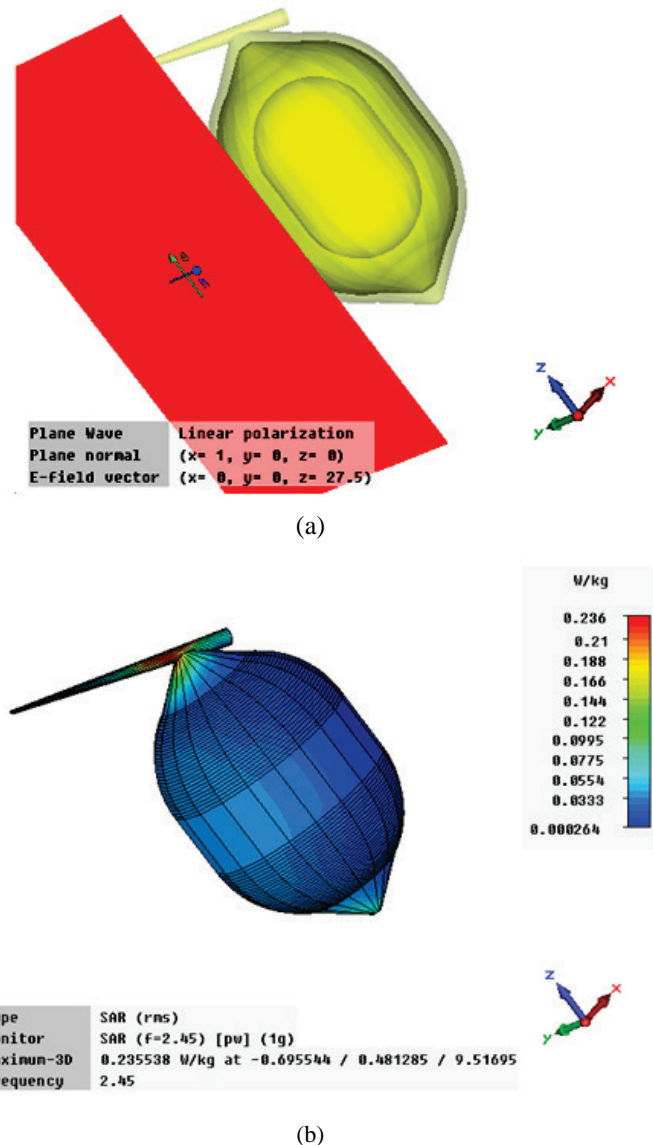


Fig. 6 (a) 2450 MHz linearly polarized plane wave (with peak E-field 27.46 V/m) impinges and passes through the twig connected coconut structure. (b) 1-g averaged SAR distribution on 3-D surface of the twig connected coconut structure at 2450 MHz in present Indian scenario

scale. SAR data have been calculated over point, 1-g and 10-g contiguous coconut tissue mass. A comparative overview of maximum local point SAR (MLP-SAR), 1-g averaged SAR and 10-g averaged SAR results for the twig connected coconut structure is illustrated in Table III and Fig. 5 respectively.

It is clearly visible in Fig. 5 that SAR data for twig connected coconut structure cannot be ignored even after revising Indian RF exposure standards to much stricter limits. Maximum Local Point SAR (MLP-SAR) value is 0.26 W/Kg at 947.5 MHz whereas the same increases to 0.69 W/Kg and 1.04 W/Kg respectively at 1842.5 MHz and 2450 MHz. Later on, it is made clear that MLP-SAR values are mostly near the twig that connects the coconut to *Cocos nucifera* plant. 1-g averaged SAR values for the twig connected coconut structure

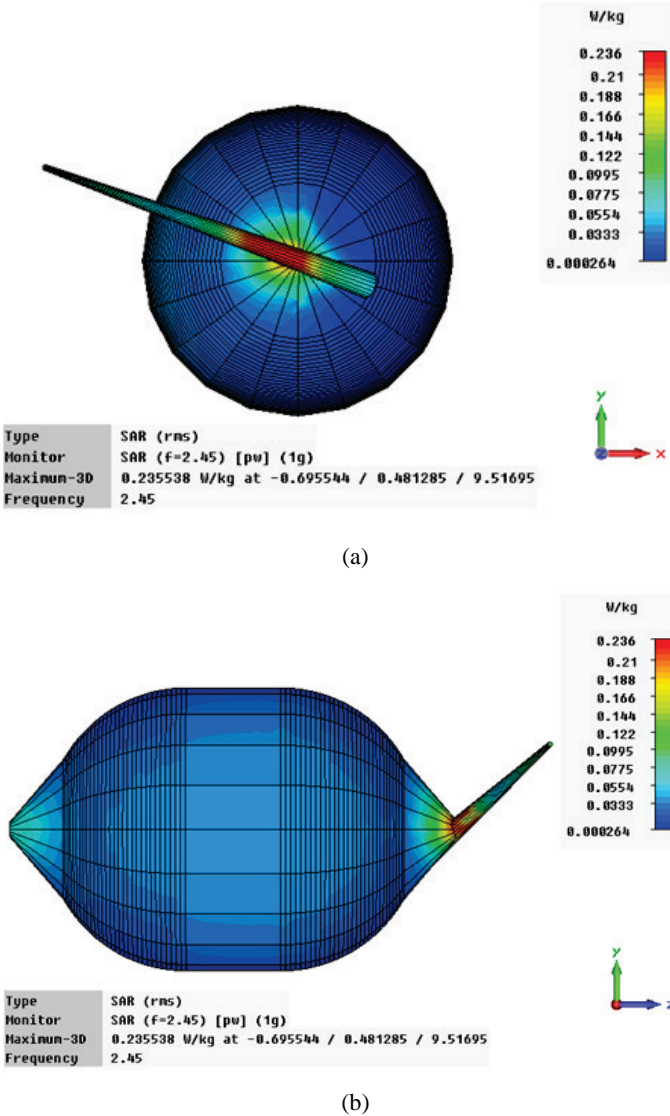


Fig. 7 (a) Top view of twig connected coconut structure illustrating 1-g averaged SAR distribution at 2450 MHz as per current Indian RF exposure standards (b) Side view of twig connected coconut structure illustrating 1-g averaged SAR distribution at 2450 MHz as per current Indian RF exposure standards

are 0.07, 0.18 and 0.24 W/Kg respectively at 947.5 MHz, 1842.5 MHz and 2450 MHz. SAR values increase at higher frequency bands mainly because of two reasons. Firstly, RF exposure level increases at higher 1800 MHz downlink band and 2400 MHz band and the same contributes to SAR increment in coconut structure. In addition, there is presence of more number of nodes and anti-nodes within the twig connected coconut structure at higher frequency bands. Free space wavelength at 1842.5 MHz is 16.28 cm but the wavelength reduces to only 1.87 cm ($\approx 16.28/76^{1/2}$) while considered in coconut water; hence there is presence of several nodes and anti-nodes within coconut water. It means that there might be some phenomenon of local temperature rise near those nodes and anti-nodes due to polar nature of coconut water content and even there might be some significant biological changes within xylem and phloem tissues of twig connected coconut fruit.

C. SAR Distribution around twig on Surface of 3D Coconut Structure at 2450 MHz

3-D SAR distributions on surface of twig connected coconut structure are illustrated in Figs. 6 and 7.

Fig. 6a illustrates that an X-direction plane wave at 2450 MHz (with E-field in Z direction as per the revised Indian RF exposure standards) impinges and passes through the twig connected coconut structure in CST-MWS 2010 simulation environment. Corresponding 1-g averaged SAR distribution on 3-D surface of the twig connected coconut structure is illustrated in Fig. 6b. 1-g averaged SAR distribution is intentionally illustrated in Fig. 6b because the revised Indian RF exposure standards prescribe restriction based on 1-g SAR averaging method only. It is clearly illustrated in Fig. 6b that MLP-SAR is distributed primarily around the twig in modified coconut structure whereas SAR values are 100 to 1000 times less on rest of the coconut surface.

1-g averaged SAR distribution is well illustrated in Figs. 7a and 7b that demonstrate top view and side view of the twig connected coconut structure respectively. In addition to Fig. 6b, illustrations in Figs. 7a and 7b validate that 1-g averaged maximum SAR location is entirely concentrated over a narrow zone around twig in this typical coconut structure. Hence, it is well established that maximum RF energy is absorbed around the junction point where twig is connected to the typical coconut structure.

V. CONCLUSION

Obtained SAR values should not be ignored especially at higher frequencies like 1842.5 MHz and 2450 MHz; the reasons for elevated SAR values at those frequencies have already been discussed earlier. It is relevant to mention that the twig contributes significantly for higher RF energy accumulation in the coconut structure due to sharp change in geometry near the junction point of twig and coconut. However while SAR averaging mass is varied from point mass to 1-g and 10-g, position of maximum 3-D SAR slightly relocates around the twig. Maximum 3-D SAR positions infer that there is a possibility of local thermal temperature rise near the junction point of twig and coconut. This temperature rise can further result in drying out the twig and consequent early fall of immature green coconuts from plant. All SAR values have been estimated only for public RF exposure zone where prescribed RF radiation densities are low enough; however, SAR values are expected to be much higher in excess and controlled RF exposure zone near base stations as prescribed RF radiation densities have not been revised by DoT, India. Moreover, It should also be noted that SAR is additive in nature for different frequencies of RF exposure; therefore, cumulative SAR in this twig connected coconut structure is expected to be much higher due to simultaneous RF exposure at different frequencies from several RF exposure sources.

An important aspect should be pointed out that coconut layers possess moderately high permittivity that contributes to store electromagnetic energy inside the coconut rather than supporting radiation from any part of the structure (example twig). Likelihood of radiation further gets minimized due to reasonable conductivity of coconut layers; it causes conversion of stored electromagnetic energy to other forms e.g. heat during multiple reflection inside the structure due to dielectric discontinuity and contributes to increase in SAR ($= \frac{\sigma E^2}{2\rho}$) value.

Finally, it should be noted that computation of 3-D SAR distribution around the twig of a realistic coconut structure is a significant novel contribution and the same is not available in literature till date [25-26]. Further biological investigations can answer queries related to probable physiological and genetic effects of RF radiation on growth of coconut fruit and plant.

ACKNOWLEDGEMENT

Authors would like to acknowledge School of Nuclear Studies and Application, Jadavpur University for providing open ended coaxial dielectric measurement kit to Microwave Engineering lab, Jadavpur University. First author would also like to acknowledge Technical Education Quality Improvement Programme (TEQIP) Phase II, Jadavpur University for granting fellowship (institute reference no.P-1/RS/196/15) during pursue of this research work.

REFERENCES

- [1] E. C Jordan and K. G. Balmain, *Electromagnetic Waves and Radiating Systems*, 2nd Edition, PHI Learning, 1964.
- [2] A. Balmori, “Pueden afectar las microondas pulsadas emitidas por las antenas de telefonía a los árboles y otros vegetales?” *Ecosistemas*, vol. 13, no. 3, pp. 79-87, 2004.
- [3] D. J. Panagopoulos, E. D. Chavdoula, and L. H. Margaritis, “Bioeffects of Mobile Telephony Radiation in Relation to its Intensity or Distance from the Antenna”, *International Journal of Radiation Biology*, vol. 86, no. 5, pp. 345-357, May 2010.
- [4] G. Kumar, “Report on Cell Tower Radiation” submitted to secretary, DoT, Delhi; December 2010.
- [5] S. Sivani, and D. Sudarsanam, “Impacts of Radio-frequency Electromagnetic Field (RF-EMF) from Cell Phone Towers and Wireless Devices on Biosystem and Ecosystem – A Review”, *Biology and Medicine*, vol. 4, no. 4, pp. 202-216, 2012.
- [6] S. S. Stuchly, M. A. Stuchly, A. Kraszewski, and G. Hartsgrove, “Energy Deposition in a Model of Man: Frequency Effects,” *IEEE Transactions on Biomedical Engineering*, vol. 33, no. 7, July 1986.
- [7] K. Meier, V. Hombach, R. Kästle, R. Y.-S. Tay, and N. Kuster, “The Dependence of Electromagnetic Energy Absorption upon Human-Head Modelling at 1800 MHz”, *IEEE Transactions on Microwave Theory and Techniques*, vol. 45, no. 11, November 1997.
- [8] A. Christ, A. Klingenbergöck, T. Samaras, C. Goiceanu, and N. Kuster, “The Dependence of Electromagnetic Far-Field Absorption on Body Tissue Composition in the Frequency Range from 300 MHz to 6 GHz”, *IEEE Transactions on Microwave Theory and Techniques*, vol. 54, no. 5, May 2006.
- [9] J. Cooper, B. Marx, J. Buhl, and V. Hombach, “Determination of Safety Distance Limits for a Human near a Cellular Base Station Antenna, Adopting the IEEE Standard or ICNIRP Guidelines”, *Bioelectromagnetics*, vol. 23, pp. 429-443, 2002.
- [10] M. A.A. Karunaratna and I. J. Dayawansa, “Energy Absorption by the Human Body from RF and Microwave Emissions in Sri Lanka”, *Sri Lankan Journal of Physics*, vol. 7, 35-47, 2006.
- [11] A. Hirata, S. Kodera, J. Wang, and O. Fujiwara, “Dominant Factors Influencing Whole-Body Average SAR Due to Far-Field Exposure in Whole-Body Resonance Frequency and GHz Regions”, *Bioelectromagnetics*, vol. 28, pp. 484-487, 2007.
- [12] A. Hirata, N. Ito, O. Fujiwara, T. Nagaoka, and S. Watanabe, “Conservative Estimation of Whole-body-averaged SARs in Infants with a Homogeneous and Simple-shaped Phantom in the GHz Region”, *Physics in Medicine and Biology*, vol. 53, pp. 7215-7223, 2008.
- [13] T. Iyama, T. Onishi, Y. Tarusawa, S. Uebayashi, and T. Nojima, “Novel Specific Absorption Rate (SAR) Measurement Method Using a Flat Solid Phantom”, *IEEE Transactions on Electromagnetic Compatibility*, vol. 50, no. 1, February 2008.
- [14] T. Wessapan, S. Srisawatdhisukul, and P. Rattanadecho, “Specific Absorption Rate and Temperature Distributions in Human Head Subjected to Mobile Phone Radiation at Different Frequencies”, *International Journal of Heat and Mass Transfer*, vol. 55, pp. 347-359, 2012.
- [15] T. Wessapan, and P. Rattanadecho, “Specific Absorption Rate and Temperature Increase in the Human Eye due to Electromagnetic Fields Exposure at Different Frequencies”, *International Journal of Heat and Mass Transfer*, vol. 64, pp. 426-435, 2013.
- [16] ICNIRP, “Guidelines for Limiting Exposure to Time-varying Electric, Magnetic and Electromagnetic Fields (up to 300 GHz)”, *Health Phys.* vol. 74, pp. 494-522 (1998).
- [17] Evaluating Compliance with FCC Guidelines for human exposure to Radio Frequency Electromagnetic Fields, *FCC OET Bulletin. 65*, Washington D.C., Aug 1997.
- [18] DoT, “Mobile Communication Radio Wave Safety,” *DoT (Delhi, India)*, 10th September 2012, Available: http://www.auspi.in/emf/02_Mobile-Communication-Radio-Waves-and-Safety-10th-sept-12-final.pdf.
- [19] H. Mazar, “A Global Survey and Comparison of Different Regulatory Approaches to Non-ionizing RADHAZ and Spurious Emissions”, *IEEE International Conference on Microwaves, Communications, Antennas and Electronics Systems (COMCAS)*, Tel Aviv, pp. 1-6, 2009.
- [20] V. Balodis, G. Brumelis, K. Kalviskis, O. Nikodemus, D. Tjarve, and V. Znotina, “Does the Skrunda Radio Location Station Diminish the Radial Growth of Pine Trees?”, *Science of The Total Environment*, vol. 180, no. 1, pp. 57-64, 2 February 1996.
- [21] I. Magone; “The Effect of Electromagnetic Radiation from the Skrunda Radio Location Station on Spirodela Polyrhiza (L.) Schleiden Cultures”, *Science of the Total Environment*, vol. 180, no. 1, pp. 75-80, 2 February 1996.
- [22] A. Balmori, “Electromagnetic Pollution from Phone Masts. Effects on Wildlife”, *Pathophysiology*, vol. 16, pp. 191-199, 2009.
- [23] D. D. Sandu, C. Goiceanu, A. Ispas, I. Creanga, S. Miclaus, D. E. Creanga, “A Preliminary Study on Ultra High Frequency Electromagnetic Fields Effect on Black Locust Chlorophylls”, *Acta Biol. Hung.*, vol. 56, pp. 109-117, 2005.
- [24] A. Kundu, B. Gupta, A. I. Mallick, and S. K. Pal, “Effects of Non-Ionizing Electromagnetic Radiation on Capsicum annuum Seed Germination and Subsequent Sapling Growth – A Time Study”, *International Conference on Microelectronics*,

- Computing and Communication (MicroCom2016)*, National Institute of Technology Durgapur, India, 23rd-25th Jan, 2016.
- [25] A. Kundu, "Study on Effects of Cell Tower Radiation on Agricultural Products", M.E. Tel. E thesis, Electronics and Tele-Communication Engineering Department, Jadavpur University, June 2013.
- [26] A. Kundu, S. B. Ray, and B. Gupta, "A Study of Specific Absorption Rate in Coconut Exposed to RF Radiation," *Microwave Review (Mikrotalasana Revija)*, vol. 20, no. 1, pp. 02-11, September, 2014.
- [27] A. Kundu, and B. Gupta, "Comparative SAR Analysis of Some Indian Fruits as per the Revised RF Exposure Guideline", *IETE Journal of Research*, vol. 60, no. 4, pp. 296-302, November 2014.
- [28] A. Kundu, "Specific Absorption Rate Evaluation in Apple Exposed to RF Radiation from GSM Mobile Towers", *IEEE Applied Electromagnetics Conference (AEMC) 2013*, KIIT University, India, 18th – 20th Dec., 2013.
- [29] A. Kundu, and B. Gupta, "SAR Evaluation of Apple as per FCC RF Exposure Guideline", *Recent Development in Electrical, Electronics & Engineering Physics (RDE3P-2013)*, MCKVIE, India, pp. 152-156, 26th-27th October, 2013.
- [30] A. Kundu, B. Gupta, and A. I. Mallick, "SAR Analysis in a Typical Bunch of Grapes Exposed to Radio Frequency Radiation in Indian Scenario", *IEEE International Conference on Microelectronics, Computing and Communication (MicroCom2016)*, National Institute of Technology Durgapur, India, 23rd – 25th Jan, 2016.
- [31] J. W.H. Yong, L. Ge, Y. F. Ng, and S. N. Tan, "The Chemical Composition and Biological Properties of Coconut (Cocos nucifera L.) Water", *Molecules*, vol. 14, no. 12, pp. 5144-5164, 2009.
- [32] CST - Computer Simulation Technology AG, *CST Microwave Studio: Workflow and Solver Overview*, 2010, <http://www.cst.com>.
- [33] M. S. Venkatesh, and G. S.V. Raghavan, "An Overview of Dielectric Properties Measuring Techniques", *Canadian Biosystems Engineering*, vol. 47, pp. 7.15-7.30, 2005.
- [34] A. P. Gregory, and R. N. Clarke, "A Review of RF and Microwave Techniques for Dielectric Measurement on Polar Liquids", *IEEE Transactions on Dielectrics and Electrical Insulation*, vol. 13, pp. 727-743, 2006.
- [35] G. Deschamps, "Impedance of an Antenna in a Conducting Medium", *IRE Transactions on Antennas and Propagation*, vol. 10, no. 5, pp. 648-650, Sept. 1962.
- [36] L. Liping, X. Deming, and J. Zhiyan, "Improvement in Dielectric Measurement Technique of Open-ended Coaxial Line Resonator Method", *Electronics Letters*, vol. 22, no. 7, pp. 373-375, March 27 1986.
- [37] X. Deming, L. Liping, and J. Zhiyan, "Measurement of the Dielectric Properties of Biological Substances Using an Improved Open-Ended Coaxial Line Resonator Method", *IEEE Transactions on Microwave Theory and Techniques*, vol. 35, no. 12, pp. 1424-1428, December 1987.
- [38] M. A. Stuchly, and S. S. Stuchly, "Coaxial Line Reflection Method for Measuring Dielectric Properties of Biological Substances at Radio and Microwave Frequencies - A Review", *IEEE Trans. Instrum. Meas.*, vol. 29, no. 3, pp 176-183, September 1980.
- [39] T. W. Athey, M. A. Stuchly, and S. S. Stuchly, "Measurement of Radio Frequency Permittivity of Biological Tissues with an Open-ended Coaxial Line: Part I", *IEEE Transactions on MTT*, vol. 30, no. 1, pp 82-86, January 1982.
- [40] M. A. Stuchly, T. W. Athey, G. M. Samaras, and G. E. Taylor, "Measurement of Radio Frequency Permittivity of Biological Tissues with an Open-Ended Coaxial Line: Part II - Experimental Results", *IEEE Transactions on Microwave Theory and Techniques*, vol. 30, no. 1, pp. 87-92, Jan. 1982.
- [41] D. M. Hagl, D. Popovic, S. C. Hagness, J. H. Booske, and M. Okoniewski, "Sensing Volume of Open-Ended Coaxial Probes for Dielectric Characterization of Breast Tissue at Microwave Frequencies", *IEEE Transactions on Microwave Theory and Techniques*, vol. 51, no. 4, April 2003.
- [42] R. Zajíček, J. Vrba, and K. Novotný, "Evaluation of a Reflection Method on an Open-Ended Coaxial Line and its Use in Dielectric Measurements", *Acta Polytechnica*, vol. 46, no. 5, 2006.
- [43] R. Zajíček, L. Oppl, and J. Vrba, "Broadband Measurement of Complex Permittivity Using Reflection Method and Coaxial Probes", *Radioengineering*, vol. 17, no. 1, April 2008.
- [44] J. S. Bobowski, and T. Johnson, "Permittivity Measurements of Biological Samples by an Open-Ended Coaxial Line", *Progress in Electromagnetics Research B*, vol. 40, pp. 159-183, 2012.